Current Science
CS 5 (3), 2687-2702 (2025)
Received 20 Feb 2025 | **Revised 20 March** 2025 | **Accepted 27 April**. 2025 | **Online Available 31 May** 2025
https://doi.org/ 10.52845/CS/2025-5-3-50

Current Science

Current Science

OPEN ACCESS

ISSN(O)2795-8639

Original Article

Single-Cell RNA-Seq Generates a Molecular Map of Affected Skin from Patients with Postherpetic Neuralgia

Zhiyou Peng[1*], Bing He[2*], Yunze Li[1*], Jinyan Huang[3#], Zhiying Feng[1#]

[1]Department of Painology, the First Affiliated Hospital, Zhejiang University School of Medicine, Hangzhou, China

[2]Department of Neuroscience, City University of Hong Kong, Hong Kong, China

[3]Biomedical Big Data Center, the First Affiliated Hospital, Zhejiang University School of Medicine, Hangzhou, China

[*]Zhiyou Peng, Bing He and Yunze Li Contributed Equally

[*]Corresponding Author: Jinyan Huang, and Zhiying Feng

Abstract:

Objective: Postherpetic neuralgia (PHN) is a prevalent complication following herpes zoster, characterized by persistent neuropathic pain. This study aimed to investigate the transcriptomic alterations in skin tissue from PHN patients, focusing on the identification of key genes and pathways involved in its pathogenesis.

Method: Full-thickness skin biopsies were obtained from both the affected areas of herpes zoster rash and their symmetrical counterparts. Differential expressed genes were identified, and functional enrichment analysis was conducted to elucidate their biological significance. Furthermore, intercellular communication among various cell types in both healthy and HZ-affected skin was analyzed. Cluster analysis was performed on skin samples from three cases of refractory PHN, comparing them to their symmetrical controls to identify distinct transcriptomic profiles.

Results: This study identified significant transcriptomic alterations in the skin samples of patients with PHN. Notably, there was a marked upregulation of CCL5, CXCL10, CXCL9, and GBP4 in monocyte cells from affected regions. In contrast, the expression of MT1G was downregulated in basal cells, while MT2a showed decreased levels in spinous cells and SPRR2E was downregulated in granular cells. GO and KEGG pathway analyses of differential expressed genes highlighted critical biological pathways and ligand-receptor interactions, particularly involving THBS, LAMININ, PTN, CD99, and FGFA, that may underlie these changes.

Conclusion: The findings from this research elucidate the transcriptomic landscape associated with PHN, revealing significant alterations indicative of early pathological processes. The observed upregulation of inflammatory markers and downregulation of protective genes suggest a complex interplay contributing to the persistence of neuropathic pain.

Key words: postherpetic neuralgia, Differential expressed genes, single-cell sequencing

1 Introduction

Herpes zoster (HZ) is caused by the reactivation of dormant varicella zoster virus (VZV) in the sensory ganglia, leading to an acutely painful vesicular rash. Postherpetic neuralgia (PHN) manifests as burning, stabbing, or sharp shooting pain with hyperalgesia or allodynia, persisting for more than three months after the rash erupts[1]. In a study of 1358 patients with acute HZ, the incidence of PHN was 9% at 6 months of HZ onset [2]. The pathogenesis of PHN may involve neuroinflammation, loss of axons and myelin sheath in sensory nerve roots, and central sensitization [3,4]. However, the exactly

pathological mechanisms that have not been fully elucidated make the clinical treatment of PHN challenging.

Gene sequencing and bioinformatics analysis have been widely used to investigate the molecular mechanisms of refractory diseases. Transcriptomics can identify key genes related to disease onset and progression, serving as an effective tool for discovering new diagnostic or therapeutic targets. Previous studies have identified multiple Differential expressed genes (DEGs) in dorsal root ganglion (DRG) sequencing data, including the abnormal expression of calcitonin gene-related peptide (CGRP) and transient receptor potential vanilloid receptor 1 (TRPV1) in a PHN rat model using VZV[5][6]. Additionally, several abnormally expressed miRNAs and circRNAs have been found in the skin lesions of PHN patients, with target mRNAs significantly enriched in 85 pathways, including AMP-activated protein kinase (AMPK) and Mitogen-activated protein kinase (MAPK) pathways[7]. Differential expression of inflammatory factors such as IL-1α has also been observed between PHN-affected skin and normal skin[8].

Keratinized skin cells, immune cells and microorganisms all interact to maintain the skin's physical and immune barriers under multiple stresses such as injury or infection[9]. Neuroimmune interactions between the sensory nervous system and the cutaneous immune system are critical in homeostasis and disease states. Currently, there are several effective topical medications used to treat peripheral neuropathic pain, including lidocaine patches, high-concentration capsaicin (8%) patches, and botulinum toxin type A. Although these drugs may target the underlying mechanisms of peripheral sensitization, the potential role of skin immune cells is unclear [10].

To explore the mechanisms underlying PHN, this study conducted a single-cell mRNA transcriptome analysis of the affected skin in PHN patients. We compared the mRNA profiles of the affected and healthy skin tissues from these patients, aiming to identify key genes and signaling pathways involved in the pathogenesis of PHN. Our goal was to provide new targets for PHN treatment.

Materials and methods

Study Design and Participants

The processes were approved by the research ethics committee of the First Affiliated Hospital, School of Medicine, Zhejiang University (IIT2021049). All subjects provided written informed consent. All methods were carried out in accordance with relevant guidelines and regulations of the First Affiliated Hospital, School of Medicine, Zhejiang University.

The inclusion criteria were as follows: (1) pain originating from HZ and the pain area is consistent with the herpes area; (2) numerical rating scale (NRS) score ≥ 4 before enrollment after routine treatment.

The exclusion criteria were as follows: (1) Patients with severe complications of brain, heart, lung, liver, kidney and other important organs; (2) Patients with skin infection or systemic infection.

Collection of Epidermal Samples

After we marked the skin of the HZ rash with hyperpigmentation and its symmetry respectively, 1% lidocaine solution 2ml was subcutaneously infiltrated anesthetized, and biopsy procedures were performed by an experienced clinician. The size of the skin excision specimen was 10mm×5mm (length×width) with complete full-thickness skin.

Epidermal Tissue Dissociation and Preparation

Fresh epidermal tissue was frozen and stored in sCelLiveTM tissue preservation solution (Singleron Bio Com, Nanjing, China) within half an hour after surgery. Specimens were washed three times with Hanks' balanced salt solution and then digested with 2 ml of sCelLiveTM tissue dissociation solution (Singlronon) for 15 min at 37°C using the Singleron PythoN™ automated tissue dissociation system. GEXSCOPE® erythrocyte lysate (Singlron, 2ml) was added, and cells were incubated at 25°C for 10 minutes to remove erythrocytes [17]. The solution was centrifuged at 500xg for 5 minutes and the cells were resuspended in PBS. Finally, cell viability was assessed under a microscope by staining with trypan blue (Sigma, United States).

Library Preparation and scRNA Sequencing

After a single-cell suspension (1 x 10^5 cells/ml) containing PBS was load into the microfluidic

device, scRNA-seq libraries were constructed according to the experimental requirements of the GEXSCOPE® Single Cell RNA Library Kit (Singlemon). Individual libraries were diluted to 4 nM and pooled for sequencing. Finally, the library was sequenced on a Novaseq6000.

Identification of Differential Expressed Genes

The screening criteria for differential mRNAs in this study were: under the screening conditions of "|avg_log2FC| > 0.5", "p_val_adj < 0.01" and "pct > 0.1"[11].

Functional Enrichment Analysis

ClusterProfiler software was applied to perform functional enrichment analysis on gene sets to explore biological functions or pathways significantly associated with specific expressed genes [12]. The significance of the KEGG pathway enrichment was determined using the same statistical approach as the GO analysis, with a p-value threshold of 0.05 for the KEGG pathway enrichment and a p-value threshold of 0.01 for the GO analysis.

Statistical Analyses

SPSS 20.0 software package (SPSS, Chicago) was used for statistical analysis. All data are expressed as mean ± standard deviation. Analysis of variance (ANOVA) and Student-Newman-Keuls q test were used to compare the values between the groups. P <0.05 was considered statistically significant.

Results

Patient Characteristic

Three patients were enrolled in this study, all with herpes zoster (HZ) affecting the thoracic dermatomes. Detailed patient demographics, including gender, age, side of the body affected, disease duration, HZ dermatomes, and BMI, along with preoperative assessment results, are summarized in Table 1.

Table 1 Patient Demographics

	Case 1	Case 2	Case 3
Age(years)	72	79	84
Sex	Male	Female	Female
Side	Left	Right	Left
Dermatome	T6-7	T4-5	T10-11
Course of HZ(months)	4	3	4
BMI	24.2	25.6	25.8
NRS	4	4	5
ID pain	4	4	4
PHQ-9	8	6	8
GAD-7	3	2	2

Pain intensity was assessed using the Numeric Rating Scale (NRS), neuropathic pain was evaluated with the ID Pain questionnaire, and anxiety and depression were measured using the GAD-7 and PHQ-9 scales, respectively.

Composition of Various Types of Cells in the Skin

To study cell diversity, we performed cluster analysis on skin samples from three patients with HZ, identifying 62,870 cells across 10 subgroups. These included monocyte DCs, sweat gland cells, pericytes, fibroblasts, endothelial cells, melanocytes, vellus hair follicle cells, granular cells, spinous cells, and basal cells (Figures 1, 2a, 2b). The proportional distribution of each cell cluster by individual sample is shown in Figure 2b.

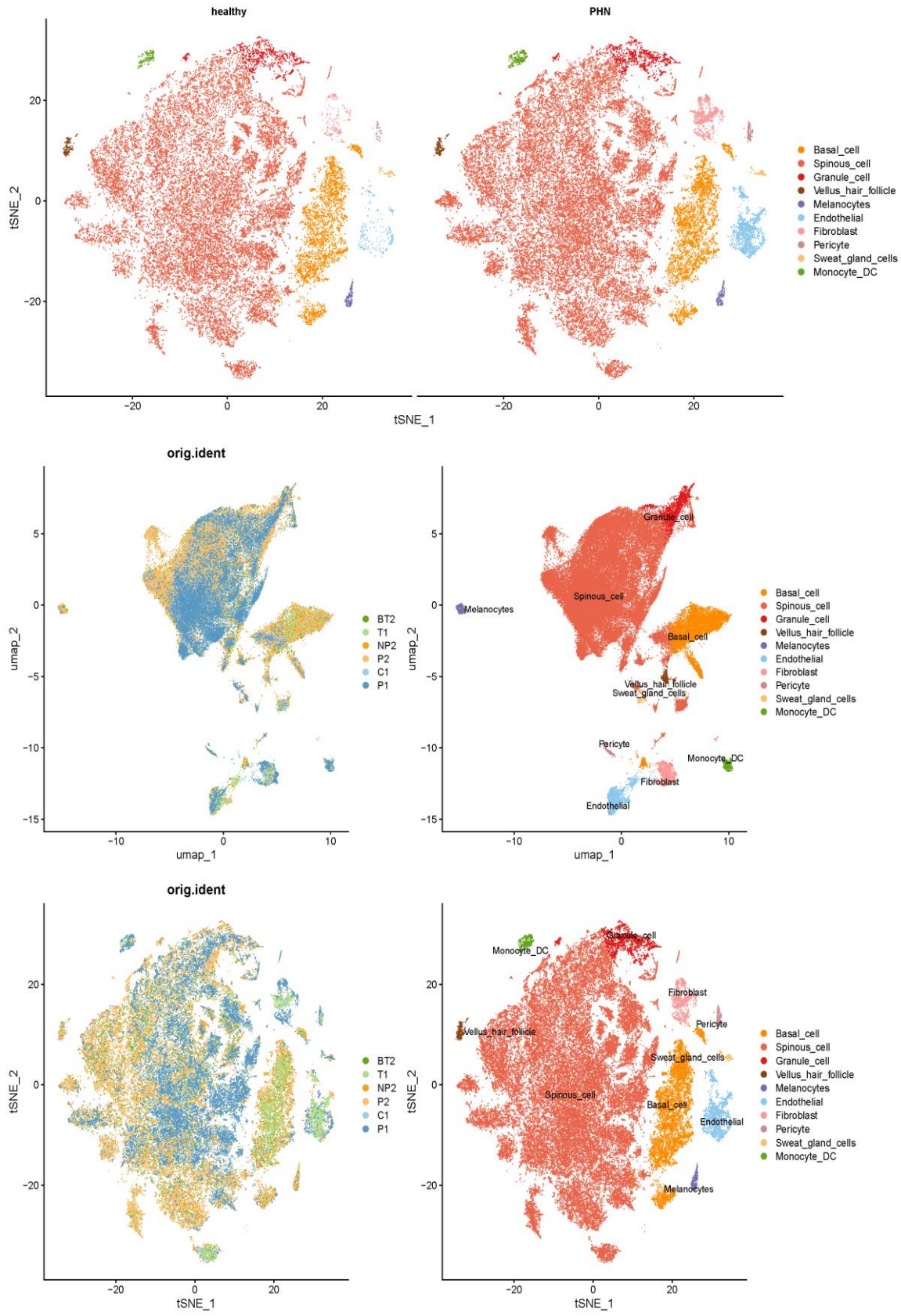
healthy
PHN
tSNE_2
tSNE_1
Basal_cell
Spinous_cell
Granule_cell
Vellus_hair_follicle
Melanocytes
Endothelial
Fibroblast
Pericyte
Sweat_gland_cells
Monocyte_DC
orig.ident
umap_2
umap_1
BT2
T1
NP2
P2
C1
P1
Granule_cell
Spinous_cell
Melanocytes
Basal_cell
Vellus_hair_follicle
Sweat_gland_cells
Pericyte
Monocyte_DC
Fibroblast
Endothelial
orig.ident
tSNE_2
tSNE_1
Monocyte_DC
Granule_cell
Fibroblast
Pericyte
Vellus_hair_follicle
Sweat_gland_cells
Spinous_cell
Basal_cell
Endothelial
Melanocytes

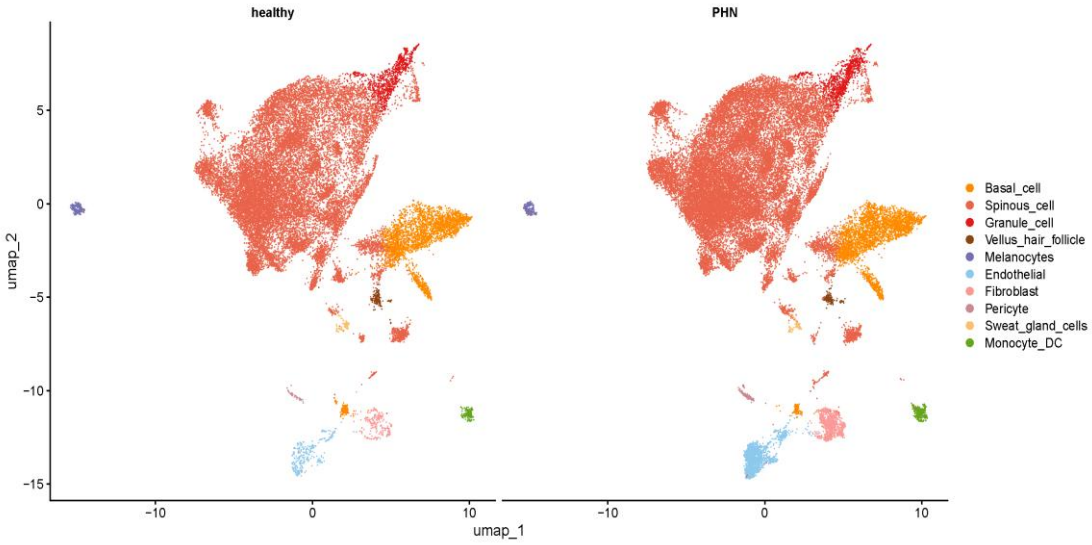

Figure 1 Color clustering UMAP by cell type (total cell)

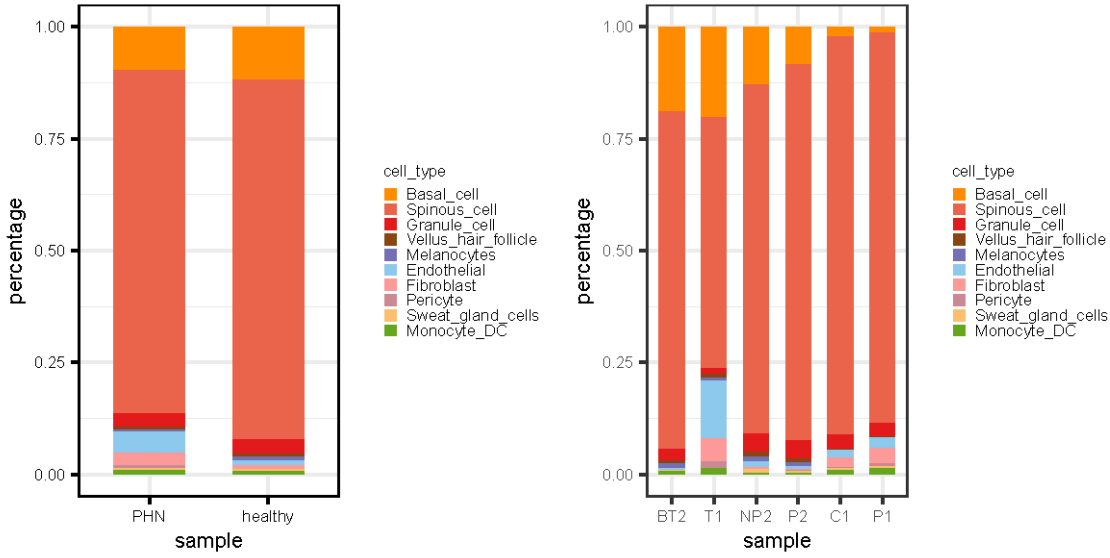

a b

Figure 2 a: A single sample of cells forms a bar diagram (total cell); b: Proportional distribution of each cell cluster by individual sample

Single cells were isolated from the affected skin samples and the symmetrical healthy skin samples of three refractory PHN patients, and their gene expression profiles were analyzed. These cells were clustered into 10 types based on marker gene expression, such as *KRT14* and *KRT5* for basal cells. The full dataset includes monocyte_DC (*PTPRC*, *LYZ*, *AIF1*), sweat gland cells (*SCGB1D2*), pericytes (*ACTA2*), fibroblasts (*DCN*), endothelial cells (*CLDN5*), melanocytes (*DCT*, *TYR*), vellus hair follicle cells (*KRT6B*), granular cells (*KRT10*, *FLG*), spinous cells (*KRT1*, *KRT10*), and basal cells (*KRT14*, *KRT5*) (Figure 3).

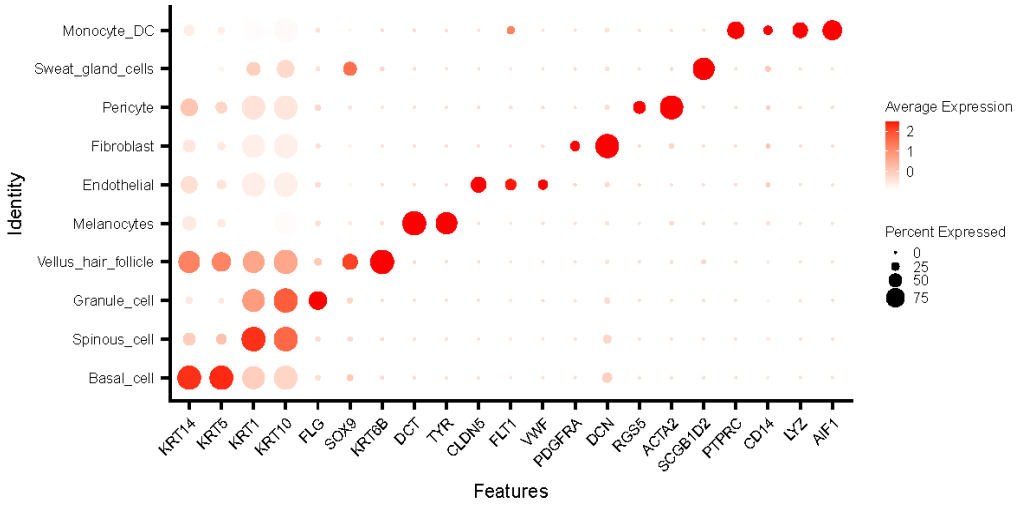

Figure 3 Cell identification and clustering.
Overview of high-expression genes for each cell type.

Differential Expressed Genes between PHN and Healthy

Single-cell RNA sequencing was performed on monocytes, granular cells, basal cells, and spinous cells from the affected and contralateral epidermis of PHN patients. Our results revealed significant differential gene expression between the PHN and healthy sides.

In monocytes, the expression of *CCL5, CXCL10, CXCL9*, and *GBP4* mRNA was upregulated, accounting for more than 5%, 10%, 5%, and 10% of the monocyte cells on the PHN side, respectively (Figure 4a). In granular cells, *SPRR2E* mRNA showed downregulated expression in more than 5% of cells on the PHN side, while upregulated expression was observed in more than 20% of cells on the healthy side (Figure 4b). In basal cells, *MT1G* mRNA was downregulated in more than 20% of cells on the PHN side and upregulated in more than 30% of cells on the healthy side (Figure 4c). In spinous cells, *MT2A* mRNA was downregulated in more than 40% of cells on the PHN side and upregulated in more than 60% of cells on the healthy side (Figure 4d).

a

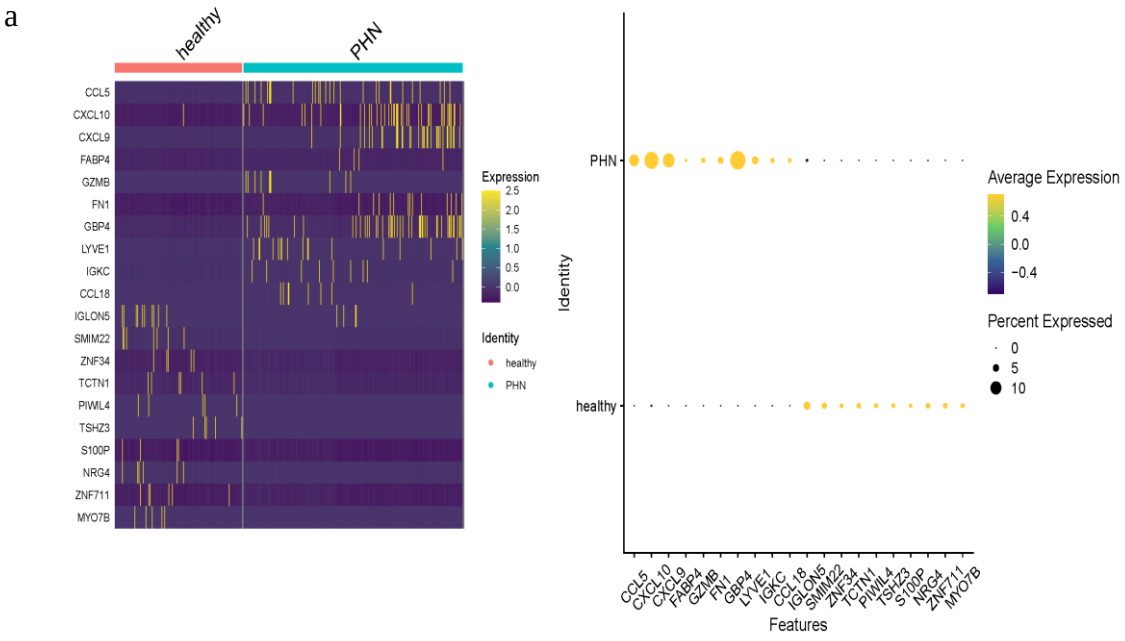

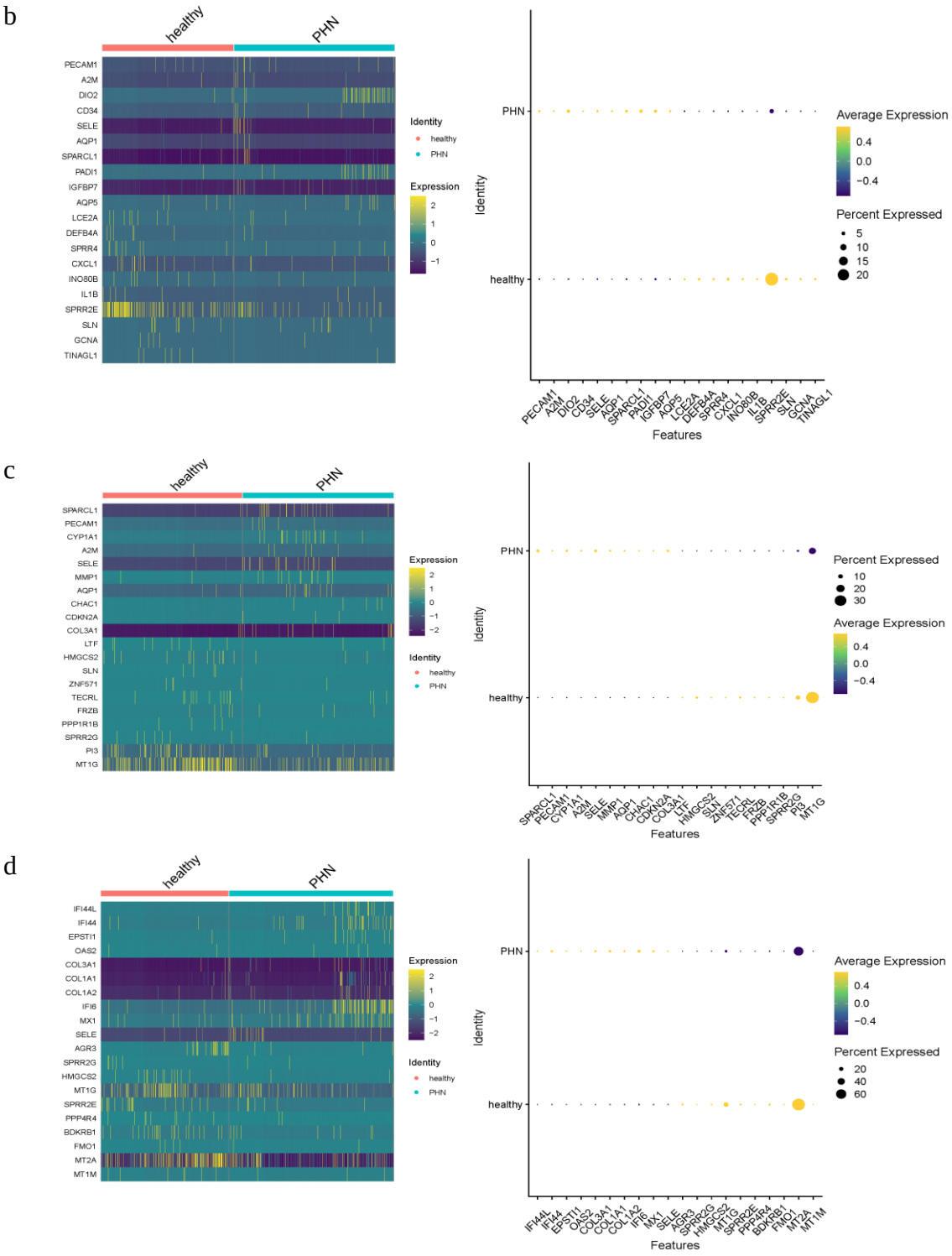

Figure 4 Differential gene expression of PHN and healthy side. a(monocyte): CCL5,CXCL10,CXCL9 and GBP4 mRNA with up-regulated expression accounted for more than 5%, 10% ,5%, 10% of the cells respectively. b(granule cell): SPRR2E mRNA with down-regulated expression accounted for more than 5% of the cells in PHN side, whereas up-regulated expression accounted for more than 20% of the cells in health side. c(basal cell): MT1G mRNA with down-regulated expression accounted for more than 20% of the cells in PHN side, whereas up-regulated expression accounted for more than 30% of the cells in health side. d(spinal cell): MT2A mRNA with down-regulated expression accounted for more than 40% of the cells in PHN side, whereas up-regulated expression accounted for more than 60% of the cells in health side. The size of the dot corresponds to the percentage of cells expressing the gene. The color represents the average level of expression. Blue means down and yellow means up. PHN: postherpetic neuraligia.

Gene Function Difference between PHN and Healthy

Differential expressed genes were classified by GO function. The top ten biological processes in monocyte cells included leukocyte activation, regulation of immune response, adaptive immune response, inflammatory response, immune effector process, lymphocyte activation, positive regulation of immune response, regulation of cell activation, regulation of leukocyte activation, and cytokine production.

The top ten cellular components included the side of the membrane, external side of the plasma membrane, cell surface, secretory vesicle, secretory granule, lysosome, lytic vacuole, vacuole, plasma membrane protein complex, and secretory granule membrane. The top ten molecular functions included molecular transducer activity, signaling receptor activity, transmembrane signaling receptor activity, immune receptor activity, molecular function activator activity, nucleoside-triphosphatase regulator activity, GTPase regulator activity, antigen binding, cytokine receptor binding, and cytokine receptor activity (Figure 5a).

The top ten biological processes, cellular components and molecular functions in Granule cells were shown in Figure 5b.

The top ten biological processes, cellular components and molecular functions in Basal cells were shown in Figure 5c.

The top ten biological processes, cellular components and molecular functions in Spinouscell cells were shown in Figure 5d.

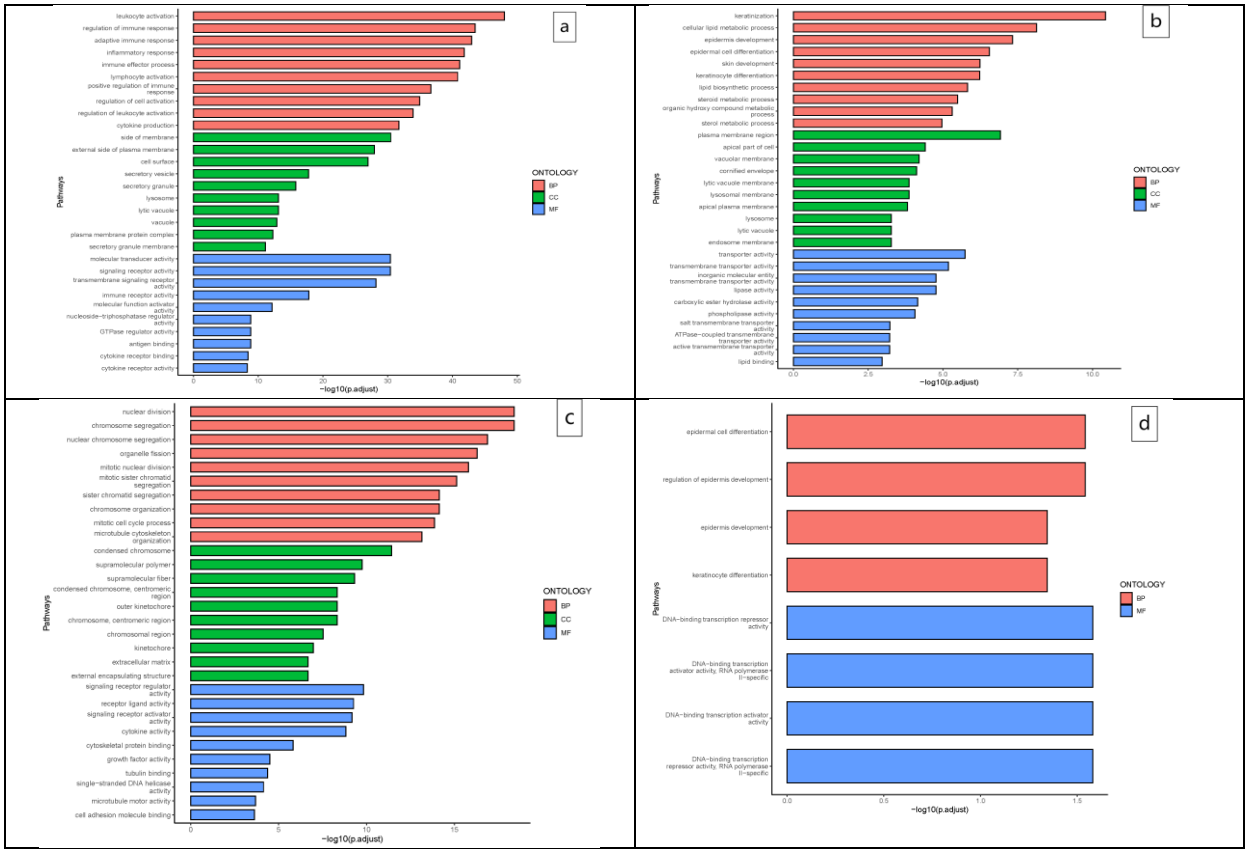

Figure 5 Functional enrichment of gene ontology (GO) in Monocyte DC cell (a), Granule cell (b), Basal cell (c), Spinouscell(d) with Differential up-regulated expression.
In the figure, the vertical axis is the name of the gene signaling pathway, and the horizontal axis is the enrichment value, which is represented by the negative logarithm of the adjusted p value (-log10). BP: biological process, CC: cellular component, MF: molecular function.

Pathway Altered in PHN

KEGG pathway enrichment analysis of monocyte DCs showed that Differential expressed genes (DEGs) in the healthy group and PHN group were enriched in six pathways, including Ribosome, Coronavirus disease-COVID-19, Hematopoietic cell lineage, Asthma, Viral myocarditis, and

Epstein-Barr virus infection (Figure 6a, left side). DEGs in the PHN group were enriched in six pathways, including Coronavirus disease-COVID-19, Viral myocarditis, Epstein-Barr virus infection, Kaposi sarcoma-associated herpesvirus infection, Antigen processing and presentation, and Chagas disease (Figure 6a, right side).

KEGG pathway enrichment analysis of spinous cells showed that DEGs in the healthy group and PHN group were enriched in three pathways: Ribosome, Coronavirus disease-COVID-19, and Mineral absorption (Figure 6b, left side). DEGs in the PHN group were enriched in five pathways: cAMP signaling pathway, TNF signaling pathway, Growth hormone synthesis, secretion and action, Renin secretion, and Amphetamine addiction (Figure 6b, right side).

KEGG pathway enrichment analysis of basal cells showed that DEGs in the healthy group and PHN group were enriched in five pathways: Ribosome, Coronavirus disease-COVID-19, Oxidative phosphorylation, Thermogenesis, and Non-alcoholic fatty liver disease (Figure 6c).

KEGG pathway enrichment analysis of granular cells showed that DEGs in the healthy group and PHN group were enriched in two pathways: Ribosome and Coronavirus disease-COVID-19 (Figure 6d, left side). DEGs in the PHN group were enriched in five pathways: Apoptosis, Estrogen signaling pathway, MAPK signaling pathway, Amphetamine addiction, and Glioma (Figure 6d, right side).

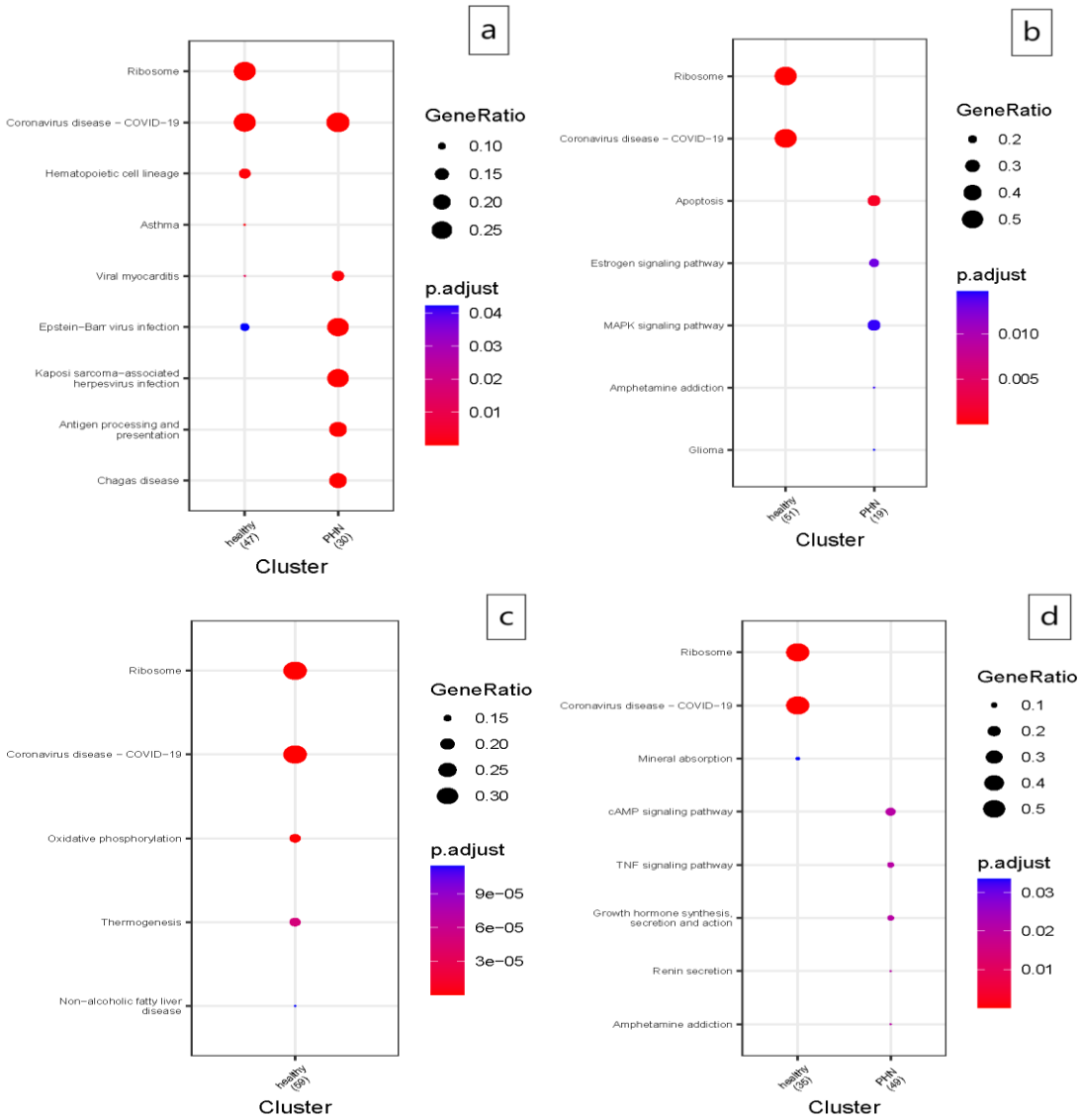

Figure 6 KEGG pathway enrichment analyses of the up-regulated DEGs in the Healthy and PHN group. Monocyte DC cell (a), Granule cell (b), Basal cell (c), Spinouscell(d). KEGG Kyoto Encyclopedia of Genes and Genomes, DEGs Differential expressed genes

Cell-cell Communication in PHN

We used CellChat [13, 14], an R toolkit that contains a database of validated human molecular interactions between signaling ligands and receptors, to predict intercellular communication in the skin samples from the healthy group and PHN group. Our analysis revealed fewer and generally weaker intercellular communication interactions in the PHN group compared to the healthy group (585 vs. 575 interactions; 11,885 vs. 9,692 interaction strength) (Figure 7A).

Fibroblasts were the major signaling sources in both groups. Endothelial cells and monocyte DCs were the dominant signaling targets in both groups. In the healthy group, the highest number of interactions occurred between fibroblasts and other cells, followed by spinous cells and other cells (Figure 7B). In the PHN group, fibroblasts showed the highest number of interactions with other cells (Figure 7B).

We compared the number of interactions and interaction strength among different cell populations to identify significant changes. In the PHN condition, signal strength from fibroblasts to basal cells and vellus hair follicles increased, while signals from fibroblasts to spinous cells and other fibroblasts decreased (Figures 7C and 7D).

A comprehensive analysis of signaling pathways revealed that, in the PHN condition, *THBS*, *PTN*, and *CD99* signaling from fibroblasts to basal cells, vellus hair follicles, and spinous cells decreased, whereas LAMININ signaling from fibroblasts to basal cells and vellus hair follicles increased (Figure 7E). Additionally, PHN induction altered *EGF*, *COLLAGEN*, *THBS*, *PTN*, and *CD99* signaling across many cell populations (Figure 7F).

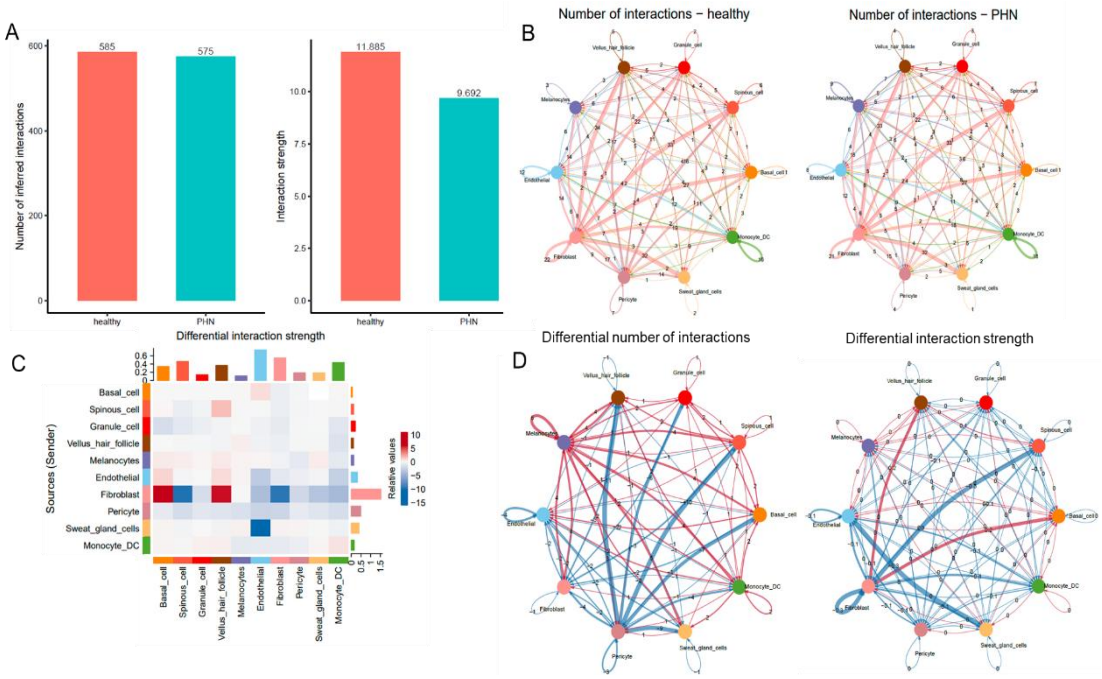

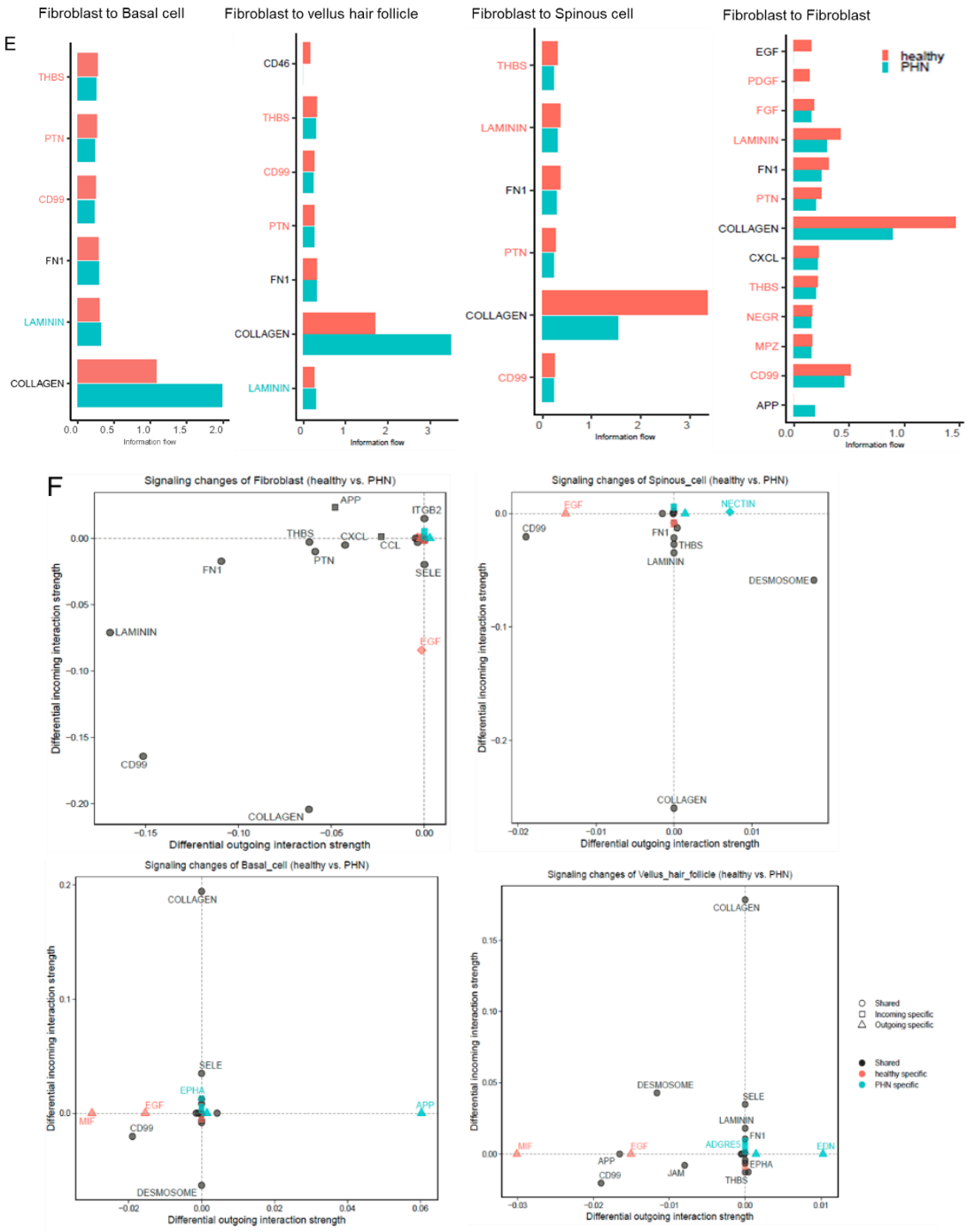
E
Fibroblast to Basal cell
Fibroblast to vellus hair follicle
Fibroblast to Spinous cell
Fibroblast to Fibroblast
healthy
PHN
Information flow
F
Signaling changes of Fibroblast (healthy vs. PHN)
Signaling changes of Spinous_cell (healthy vs. PHN)
Signaling changes of Basal_cell (healthy vs. PHN)
Signaling changes of Vellus_hair_follicle (healthy vs. PHN)
Differential incoming interaction strength
Differential outgoing interaction strength
Shared
Incoming specific
Outgoing specific
Shared
healthy specific
PHN specific

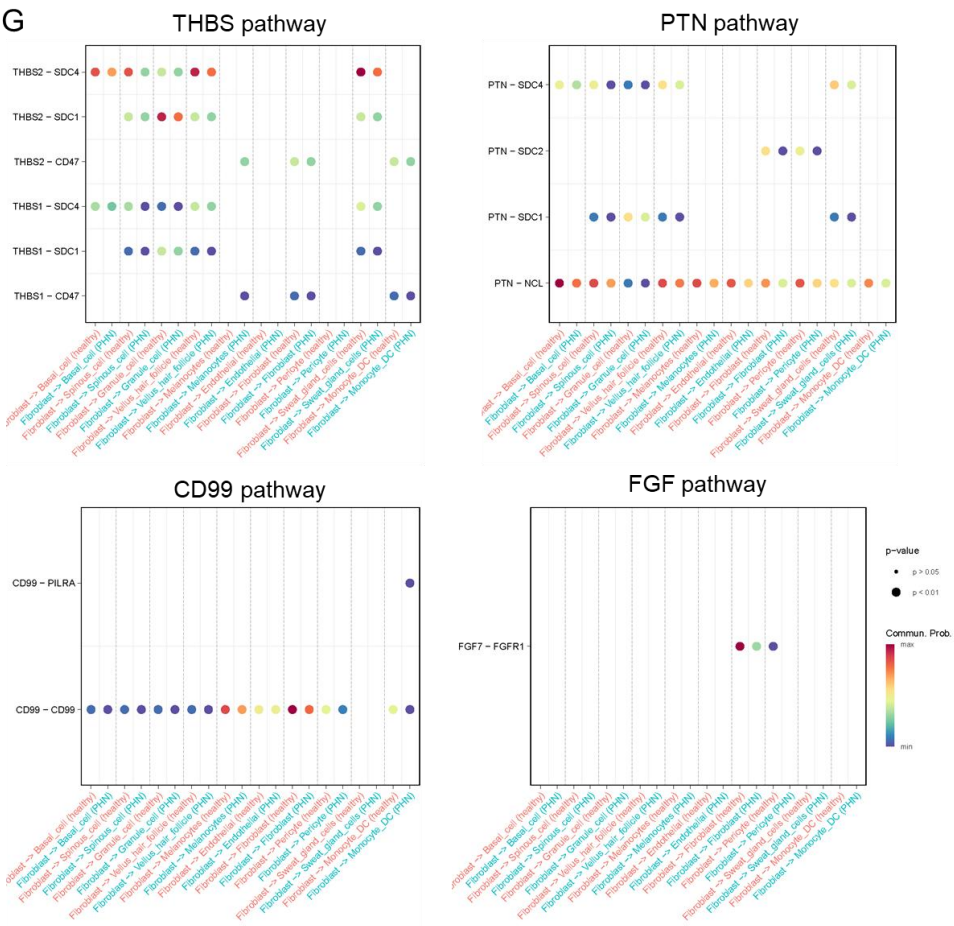

Figure 7 Analysis of intercellular communication among various cell types in the healthy group and PHN group.

(A) Bar graph illustrating the quantity and strength of cell communication between the healthy group and PHN group; inferred cell-cell communication network is reduced in the PHN group.

(B)The differential number of interactions and interaction strength between any 2 cell populations in the healthy group and PHN group. Red (or blue) colored edge lines represent increased (or decreased) signaling in the PHN compared to the healthy group.

(C) Scatter plot of incoming and outgoing interaction strength of each cell population in the healthy group and PHN group.

(D) Heatmap of differential interaction strength in PHN compared to the healthy group. The top-colored bar plot represents the sum of column of values displayed in the heatmap (incoming signaling). The right-colored bar plot represents the sum of row of values (outgoing signaling). In the heatmap, red (or blue) represents increased (or decreased) signaling in PHN compared to healthy group. Relative value = the communication probability from source to target in PHN group—the communication probability from source to target in healthy group.

(E) Information flow numbers between major cell types in the healthy and PHN groups.

(F) 2D visualization of differential outgoing and incoming signaling changes of major cell types in PHN group compared to healthy group.

(G) Bubble plot of the communication probabilities of all the significant ligand-receptor pairs that contributed to THBS, LAMININ, PTN, CD99 and FGFA pathway between group and PHN group. Dot color reflects communication probabilities and dot size represents computed p-values. Space means the communication probability is zero.

Discussion

In urban China, PHN is associated with significant patient-reported burdens, affecting sleep, quality of life, and daily activities, including work impairment. This underscores the need for further optimization of PHN prevention and management strategies[1, 15]. First-line treatments for PHN include tricyclic antidepressants, gabapentin, pregabalin, and the topical lidocaine 5% patch. Interventional pain management options such as epidural steroid injections, dorsal root ganglion radiofrequency ablation, and spinal cord stimulators are also effective[16, 17]. Despite these options, PHN treatment remains challenging for clinicians. Therefore, exploring the molecular mechanisms of PHN to identify better therapeutic targets is of great clinical significance[18].

Previous genomic and proteomic studies on PHN have primarily focused on the dorsal root ganglia and spinal cord tissues in animal models, with few studies examining the skin samples of PHN patients[19, 20]. The skin, a complex protective network, is crucial in neuroimmune interactions[21], particularly under the neuroepidermal tropism of varicella-zoster virus, which causes neurogenic inflammation and immunity-related disorders along the affected dermatome[22]. Evidence of HZ-related cutaneous neural injury supports the role of skin inflammation in PHN pathogenesis[23]. For instance, a study showed that skin excision in a patient with longstanding PHN reduced pain, eliminated tactile allodynia, and decreased medication use over a year[24] [25].

Our study yielded several significant findings. We observed upregulated expression of *CCL5*, *CXCL10*, *CXCL9*, and *GBP4* mRNA in monocyte cells on the PHN side. Conversely, SPRR2E mRNA was downregulated in granular cells on the PHN side and upregulated on the healthy side. *MT1G* mRNA was downregulated in basal cells on the PHN side and upregulated on the healthy side, while *MT2A* mRNA was downregulated in spinous cells on the PHN side and upregulated on the healthy side.

The downregulation of SPRR2E and MT1G in keratinocytes (KCs) may be attributed to a maladaptive response to chronic inflammation in the skin associated with postherpetic neuralgia (PHN). SPRR2E, a member of the small proline-rich protein family, plays a critical role in cellular stress responses and is involved in maintaining skin barrier integrity. Its downregulation could impair the skin's protective barrier, making it more susceptible to inflammation and further contributing to chronic pain states.Evidence suggests that similar mechanisms are at play in other tissues, such as biliary epithelial cells (BECs), where SPRR2 expression is regulated by IL-6/gp130/STAT3 signaling in response to stress [26][27]. In this context, the noncoordinate upregulation of SPRR2 has been shown to contribute to the functional integrity of the biliary barrier following injury[27]. This parallels the potential implications of SPRR2E downregulation in KCs, where compromised barrier function due to reduced SPRR2E expression may exacerbate inflammatory responses.

Moreover, MT1G, a metallothionein gene involved in metal ion homeostasis and oxidative stress response, is similarly downregulated in various conditions, including gastric cancer, where its decreased expression correlates with increased oxidative stress and ferroptosis. In gastric cancer cells, overexpression of MT1G has been shown to inhibit proliferation and migration while promoting autophagy and iron metabolism through the GPX4/SQSTM1 axis, highlighting its protective role in cellular stress response[28]. This downregulation in KCs may lead to increased cellular vulnerability and altered pain signaling pathways. Together, these changes in KCs may exacerbate the inflammatory environment in PHN-affected skin, contributing to the persistence of neuropathic pain.

Among these, the upregulation of *CCL5*, *CXCL10*, *CXCL9*, and *GBP4* mRNA in monocyte cells of PHN-affected skin was particularly notable. *CXCL9, CXCL10, CXCL11*, and *CCL5*, typically secreted by M1 macrophages, recruit Th1, Th17, and cytotoxic T cells, playing critical roles in tissue homeostasis and inflammation by responding to tissue damage and infection[29]. These chemokines control inflammation and immune responses through leukocyte migration, making them potential diagnostic indicators or therapeutic targets in inflammatory diseases[30].

Previous studies have shown that multiple types of inflammation are driven by the abnormal interaction of CCL5/CCR5, leading to conditions such as hepatitis, atherosclerosis, and microglia

inflammation. The chemotaxis of *CCL5/CCR5* initiates CD4+/CD8+ T cell-mediated immunity, NK cell migration, and macrophage infiltration into infected tissues[31]. Wu et al. identified CCR5 as a therapeutic target for alleviating HSV-1 infection-induced HN, demonstrating that blocking CCR5 reduced allodynia and hyperalgesia by suppressing inflammatory cytokines in the DRG and spinal cord[20].

Our single-cell transcriptomic analysis revealed significant alterations in the mRNA expression profile of the affected skin in PHN patients. GO and KEGG analyses indicated that upregulated genes in the affected skin were predominantly related to *CCL5*, *CXCL10*, *CXCL9*, and *GBP4* mRNA in monocyte cells, providing valuable candidates for future PHN research.

Additionally, our study investigated intercellular communication among various cell types in healthy individuals and PHN patients. We found a reduced and weaker intercellular communication network in the PHN group compared to the healthy group. Fibroblasts were the major signaling sources in both groups, with endothelial and monocyte DCs as the primary signaling targets. The highest number of interactions in PHN was found between fibroblasts and other cells.

Our analysis indicated that THBS, PTN, and CD99 signaling from fibroblasts to basal cells, vellus hair follicles, and spinous cells decreased in the PHN condition, while LAMININ signaling increased. PHN induction altered EGF, COLLAGEN, THBS, PTN, and CD99 signaling across many cell populations. The analysis of outgoing THBS, PTN, CD99, and FGF signaling from fibroblasts revealed several ligand-receptor pairs with high communication probabilities in the healthy state, including THBS2-SDC4, PTN-NCL, CD99-CD99, and FGF7-FGFR1. Our results also highlighted specific pathways and ligand-receptor pairs, such as THBS, LAMININ, PTN, CD99, and FGFA, which may play important roles in PHN. For example, while the THBS2-SDC4 pathway has not been extensively studied in PHN, previous research indicated that Thbs2 is downregulated in a neuropathic pain rat model treated with diclofenac sodium, suggesting its importance in maintaining skin homeostasis[32]. Overall, these findings exemplify how PHN may alter intercellular communication among various cell types, providing new insights into altered communication patterns in PHN with implications for diagnosis and treatment.

In light of recent findings from a study comparing blood transcriptomics of PHN patients with Herpes zoster (HZ) patients, our results further elucidate the distinctive transcriptomic alterations present in PHN. While that study suggested a reduced overall expression level in PHN compared to Herpes zoster (HZ), our work highlights specific upregulated chemokines in monocytes that could indicate an ongoing inflammatory response and immune dysregulation unique to PHN. This comparison underscores the need to integrate our findings with existing literature to determine how these alterations contribute to PHN's clinical manifestations and progression from HZ[33].

This study acknowledges several limitations. Firstly, while transcriptomic alterations in the skin of PHN patients were identified, the causal relationship between these changes and the onset of pain remains unclear. It is uncertain whether the observed transcriptomic shifts are a consequence of pain or if they contribute to the progression from herpes zoster to PHN. Secondly, to enhance the robustness of our findings, a larger cohort is essential. Ideally, this should involve RNA sequencing (RNA-Seq) followed by quantitative reverse transcription PCR (qRT-PCR) to accurately assess the expression levels of key shortlisted genes. Lastly, validation of certain findings at the protein level is critical to confirm the biological significance of the identified transcriptomic changes. However, due to the challenges in obtaining sufficient tissue samples and the complexity of protein interactions in the skin environment, this validation remains a key area for future research.

In conclusion, our findings provide valuable insights into the distinct cellular populations and gene expression profiles present in the skin of healthy and PHN groups. This research may illuminate critical biological mechanisms and pathways associated with PHN, thereby informing more effective treatment strategies for affected patients.

Declarations

Acknowledgments

This study was supported by the National Natural Science Foundation of China (No. 82271239), and the Joint Funds of the Zhejiang Provincial Natural Science Foundation of China (No. LBY23H110001).

Conflict of Interest statement

The authors confirm that there are no conflicts of interest.

Data Availability

The datasets are available from the corresponding author on reasonable request.

References:

1. Salleras, L., et al., Herpes zoster and postherpetic neuralgia in Catalonia (Spain). Hum Vaccin Immunother, 2015. 11(1): p. 17 8-84.
2. Bouhassira, D., et al., Patient perspective on herpes zoster and its complications: an observational prospective study in patients aged over 50 years in general practice. Pain, 2012. 153(2): p. 342-349.
3. Schlereth, T., et al., Association between pain, central sensitization and anxiety in postherpetic neuralgia. Eur J Pain, 2015. 19(2): p. 193-201.
4. Sommer, C., M. Leinders and N. Uceyler, Inflammation in the pathophysiology of neuropathic pain. Pain, 2018. 159(3): p. 595-6 02.
5. Guedon, J.M., et al., Neuronal changes induced by Varicella Zoster Virus in a rat model of postherpetic neuralgia. Virology, 2015. 482: p. 167-80.
6. Wu, S., et al., Transcriptome Analysis Reveals the Role of Cellular Calcium Disorder in Varicella Zoster Virus-Induced Post-Herpetic Neuralgia. Front Mol Neurosci, 2021. 14: p. 665931.
7. Cao, S., et al., MicroRNA And Circular RNA Expression In Affected Skin Of Patients With Postherpetic Neuralgia. J Pain Res, 2019. 12: p. 2905-2913.
8. Cao, S., et al., Inflammatory cytokine expression in the skin of patients with postherpetic neuralgia. J Int Med Res, 2020. 48(8): p. 300060520929582.
9. Belkaid, Y. and J.A. Segre, Dialogue between skin microbiota and immunity. Science, 2014. 346(6212): p. 954-9.
10. Kocot-Kepska, M., et al., Topical Treatments and Their Molecular/Cellular Mechanisms in Patients with Peripheral Neuropathic Pain-Narrative Review. Pharmaceutics, 2021. 13 (4).
11. Grieshaber-Bouyer, R., et al., The neutrotime transcriptional signature defines a single continuum of neutrophils across biological compartments. Nat Commun, 2021. 12(1): p. 2 856.
12. Yu, G., et al., clusterProfiler: an R package for comparing biological themes among gene clusters. OMICS, 2012. 16(5): p. 284-7.
13. Jin, S., et al., Inference and analysis of cell-cell communication using CellChat. Nat Commun, 2021. 12(1): p. 1088.
14. He, H., et al., Single-cell transcriptome analysis of human skin identifies novel fibroblast subpopulation and enrichment of immune subsets in atopic dermatitis. J Allergy Clin Immunol, 2020. 145(6): p. 1615-1628.
15. Yu, S.Y., et al., Patient and economic burdens of postherpetic neuralgia in China. Clinicoecon Outcomes Res, 2019. 11: p. 539-550.
16. Grace, P.M., et al., The Neuroimmunology of Chronic Pain: From Rodents to Humans. J Neurosci, 2021. 41(5): p. 855-865.
17. Mercan, A., et al., Immunological mechanism of postherpetic neuralgia and effect of pregabalin treatment on the mechanism: a prospective single-arm observational study. Korean J Pain, 2021. 34(4): p. 463-470.
18. Gilden, D., et al., Review: The neurobiology of varicella zoster virus infection. Neuropathol Appl Neurobiol, 2011. 37(5): p. 441-63.
19. Qiu, Y., et al., Bioinformatics Analysis of Genes and Mechanisms in Postherpetic Neuralgia. Pain Res Manag, 2020. 2020: p. 13 80504.
20. Wu, S., et al., HSV-1 infection-induced herpetic neuralgia involves a CCL5/CCR5-mediated inflammation mechanism. J Med Virol, 2023. 95(4): p. e28718.
21. Slominski, A.T., et al., Sensing the environment: regulation of local and global homeostasis by the skin's neuroendocrine system. Adv Anat Embryol Cell Biol, 2012. 2 12: p. v, vii, 1-115.
22. Ruocco, V., et al., Beyond zoster: sensory and immune changes in zoster-affected dermatomes: a review*. Acta Derm Venereol, 2012. 92(4): p. 378-82.

23. Petersen, K.L., et al., Natural history of cutaneous innervation following herpes zoster. Pain, 2010. 150(1): p. 75-82.
24. Petersen, K.L., et al., Relief of post-herpetic neuralgia by surgical removal of painful skin. Pain, 2002. 98(1-2): p. 119-26.
25. Devor, M., Rethinking the causes of pain in herpes zoster and postherpetic neuralgia: the ectopic pacemaker hypothesis. Pain Rep, 2018. 3(6): p. e702.
26. Lin, Z.Q., et al., Essential involvement of IL-6 in the skin wound-healing process as evidenced by delayed wound healing in IL-6-deficient mice. J Leukoc Biol, 2003. 73(6): p. 713-21.
27. Nozaki, I., et al., Small proline-rich proteins 2 are noncoordinately upregulated by IL-6/STAT3 signaling after bile duct ligation. Lab Invest, 2005. 85(1): p. 109-23.
28. Meng, K., et al., MT1G promotes iron autophagy and inhibits the function of gastric cancer cell lines by intervening in GPX4/SQSTM1. Sci Rep, 2024. 14(1): p. 28539.
29. Amorim, A., et al., IFNgamma and GM-CSF control complementary differentiation programs in the monocyte-to-phagocyte transition during neuroinflammation. Nat Immunol, 2022. 23(2): p. 217-228.
30. Zhou, C., et al., The role of CXCL family members in different diseases. Cell Death Discov, 2023. 9(1): p. 212.
31. Zeng, Z., et al., CCL5/CCR5 axis in human diseases and related treatments. Genes Dis, 2022. 9(1): p. 12-27.
32. Zhang, Y., et al., Diclofenac sodium nanomedicine results in pain-relief and differential expression of the RNA transcriptome in the spinal cord of SNI rats. International journal of pharmaceutics, 2024. 659: p. 124276.
33. Wang, C., et al., Exploring blood transcriptomic signatures in patients with herpes zoster and postherpetic neuralgia. Front Cell Infect Microbiol, 2024. 14: p. 1425393.